

Chapter 6

2-D Inversion of inter-station transfer functions

Since a few years, isotropic two-dimensional forward modelling of electromagnetic transfer functions can no longer be regarded as a state-of-the-art technique in explaining field data, since a number of effective 2-D inversion codes have been written, which mostly are freely available (e.g. *de Groot-Hedlin and Constable* [1990], *Siripunvaraporn and Egbert* [2000], *Rodi and Mackie* [2001]). Unfortunately, none of the commonly used codes includes an inversion of any inter-station transfer functions. Fortunately, however, an existing code can in general be expanded to the inversion of such data type, without major interference with the preexisting inversion routines. In this work, by the courtesy of the authors, the REBOCC code from *Siripunvaraporn and Egbert* [2000] was used as a frame.

6.1 General considerations . . .

6.1.1 . . . on the amount of information

As demonstrated in section 2.2, the multivariate data analysis provides an estimate of the array's response on incident uniform source fields, i.e. the two-dimensional response space \mathcal{R} , from which all possible inter-component transfer functions of the processed array can be calculated. The reflections on the indeterminacy of the response itself show that only $2m - 4$ inter-component transfer functions can be linearly independent, if m is the number of components within the array. An exhaustive modelling will aim at reproducing this response space, represented (at least) by a *complete* set of transfer functions, yielding a minimum structured (see below) estimate on the subsurface conductivity distribution.

A complete set of transfer functions could comprise the local impedance tensor \mathbf{Z} , the local geomagnetic tipper functions T_x & T_y and the geomagnetic perturbation \mathbf{W}_{hor} with respect to a chosen reference site for each station (the "-4" from above is reflected in the null-information of the perturbation at the reference). For true 2-D structures with strike direction x , a complete set of transfer functions would thus be Z_{xy}, Z_{yx}, T_y and d_D . To fit an exceeding set of *true* 2-D data (e.g. *additionally* inverting for z_D) in any forward or inverse modelling means dealing with redundancy and might be avoided in order to save computational resources. However, an expansion of the set to e.g. additional perturbation matrices

with respect to further references could eventually stabilize the modelling procedure, as the impacts of data quality and location of the reference station are reduced.

6.1.2 ... on the uniqueness of inversion solutions

Magnetotelluric and geomagnetic field data are in a strong sense not invertible, since any analytical model will always be just an abstraction of the real conductivity distribution, the number of free parameters of this abstraction in general exceeds the number of data (i.e. transfer functions), and real data are in addition always faulty. However, under idealized conditions – i.e. an infinite amount of precise data and models of mathematically well-behaved conductivity distribution – it is possible to derive mathematical proofs on uniqueness of inversion solutions and thus invertability. *Tikhonov* [1965] showed that a piecewise analytical 1-D conductivity distribution is uniquely determined by knowing the impedance as a function of frequency. *Weidelt* [1978] found an analytical proof (only for TE-mode), that also the 2-D magnetotelluric inversion problem has a unique solution. *Gusarov* [1981] formulated a uniqueness theorem for 2-D media that covers the impedances of both modes independently (*M. N. Berdichevsky, pers. comm.*). The theorem from *Weidelt* [1978] states:

Let $\sigma(y, z)$, $z > 0$ be an analytical bounded function of the variables y and z ($0 < \sigma_- \leq \sigma(y, z) \leq \sigma_+ < \infty$), which shades off into a 1-D distribution for $y \rightarrow \pm\infty$. Induced is a quasi-uniform field: $B_y(y, \omega) \rightarrow B_N(\omega)$ for $y \rightarrow \infty$. Then:

If the function $e(y, \omega) = E(y, \omega)/B_N(\omega)$ is given on the continuum (y_-, y_+) and (ω_-, ω_+) , then the conductivity distribution $\sigma(y, z)$ is determined uniquely.

After a remark from *Weidelt* [1978], $\sigma(y, z)$ was chosen analytical to simplify the proof and the analytical nature does not imply a principal restriction: the range of possible models can particularly be expanded to the class of piecewise analytical models. The author also pointed out that the proof of the theorem does by no means provide the determination of $\sigma(y, z)$. Integrating $\partial E_x/\partial y = i\omega B_z$ (from Maxwell equation 2.5b, see also eq. 2.22), and dividing it by the normal horizontal magnetic field B_N yields:

$$e(y, \omega) = Z_N(\omega) - i\omega \int_y^\infty z_D dy' \quad (6.1)$$

The Hilbert-transformation, here derived from the Maxwell equation (quasi-static approximation) $\nabla \times \mathbf{B} = \mu_0 \mathbf{j}$ (cf. *Rokityansky* [1982], p. 277) and again normalized to B_N , relates the vertical and horizontal magnetic field components to each other:

$$z_D(y) = -\frac{1}{\pi} \int_{-\infty}^\infty \frac{d_D(y')}{y' - y} dy' \quad (6.2)$$

Thus, it seems that the transfer functions d_D and z_D , if known on the continuum $(-\infty, +\infty; \omega_-, \omega_+)$, do only uniquely determine the conductivity distribution, if the normal impedance Z_N is additionally given.

Very recently, *Berdichevsky et al.* [2000] could show for the same class of models (provided that $\sigma(y, z) \neq \sigma(z)$, i.e. there is spatial conductivity variation) that the ‘local anomalous’

impedance

$$Z_{\parallel}^a(y, \omega) = \frac{E_x^a}{B_y^a} = \frac{e(y, \omega) - Z_N(\omega)}{d_D} = \frac{1}{d_D} \left(-i\omega\mu_o \int_y^{\infty} z_D(y') dy' \right) \quad (6.3)$$

approximates to $Z_N(\omega)$ for distances far away from conductivity contrasts. They give the physical explanation that the external part of the anomalous field, which is due to anomalous currents in the inhomogeneities, gets quasi uniform towards the remote zone and thus obeys the Tikhonov-Cagniard impedance relations.

Additionally, they find an iterative method to relate the transfer functions d_D and z_D to the local geomagnetic tipper T_y , provided that the former are known on the entire y-axis. Altogether, we can derive for conductivity distributions as in *Weidelt* [1978], with spatial variation of conductivity:

If any of the transfer functions related to the TE-mode ($Z_{\parallel}, T_{yz}, d_D, z_D$) is given on the entire y-axis and on the continuum (ω_-, ω_+), then the conductivity distribution is determined uniquely.

Now let D^0 be the horizontal magnetic field at a specific coordinate y^0 . Then with $D = B_N = B_y(\infty) = (1 + d_{D^0}(\infty)) * D_0$, we can write:

$$d_D(y) = \frac{d_{D^0}(y) - d_{D^0}(\infty)}{1 + d_{D^0}(\infty)} \quad (6.4)$$

$$z_D(y) = \frac{z_{D^0}(y)}{1 + d_{D^0}(\infty)} \quad (6.5)$$

As these data can be transformed into each other, the uniqueness theorem is also to valid for the transfer functions d_{D^0} and z_{D^0} (cf. Hilbert transformation in eq. 6.2) with an arbitrarily chosen reference.

6.2 The inversion scheme of the employed program

All details on the REBOCC inversion algorithm that will be described here are taken from *Siripunvaraporn and Egbert* [2000] and from thorough inspection of the source code itself. The considerations on the uniqueness of inversion solutions from above are, as pointed out, only valid for ideal data sets with analogue character, i.e. continuous in time/frequency and space. Dealing with real, discrete and faulty data implies on one hand that the misfit of each datum has to be related the corresponding uncertainty, and on the other hand that a number of models can explain the data equally well.

Let \mathbf{d} be the vector of all N data to be inverted ($\mathbf{d} = (d_1, d_2, \dots, d_N)$), and \mathbf{F} be the highly nonlinear function, yielding the synthetic response of the model \mathbf{m} , which consists of M discrete blocks of constant resistivity. Then out of the space of models, which's responses fit the measured data sufficiently well, i.e. the data misfit

$$\chi_d^2 = (\mathbf{d} - \mathbf{F}(\mathbf{m}))^T \mathbf{C}_d^{-1} (\mathbf{d} - \mathbf{F}(\mathbf{m})) \quad (6.6)$$

(where \mathbf{C}_d is the – in general diagonal – covariance matrix of the data, containing the errors) is close to a desired misfit χ_*^2 , the algorithm shall find the model with the least structure, as this is supposed to be one of high physical relevance. As a measure for the model structure, the norm

$$\chi_m^2 = (\mathbf{m} - \mathbf{m}_0)^T \mathbf{C}_m^{-1} (\mathbf{m} - \mathbf{m}_0) \quad (6.7)$$

is calculated in this code. Here, \mathbf{m}_0 is an initially defined prior model, and \mathbf{C}_m is a model covariance “characterizing the expected magnitude and smoothness of resistivity variations relative to \mathbf{m}_0 ” (see appendix of *Siripunvaraporn and Egbert [2000]* for details). Instead of a model covariance, often ‘roughness’ operators are employed, realized by matrices which act as first- or second-differences operator on the model vector containing the resistivities (e.g. *Schwaberg [2000]*).

Seeking for a model with the described qualities leads to the mathematical formalism of implicit functions and to the introduction of a Lagrange-multiplier λ , acting as a ‘trade-off’ parameter between data misfit and model norm. The preferred model is supposed to be a stationary point of the ‘penalty functional’:

$$U(\mathbf{m}, \lambda) = \chi_m^2 + \lambda^{-1}(\chi_d^2 - \chi_*^2) \quad (6.8)$$

Without the restriction to minimize the model norm, the inversion would generate erratic models with extreme variations. Since the model response function \mathbf{F} is nonlinear, the problem cannot be solved directly. Therefore, an iterative scheme has to be adopted, where $\mathbf{F}(\mathbf{m})$ is linearized by an expansion into Taylor series:

$$\mathbf{F}(\mathbf{m}_{k+1}) = \mathbf{F}(\mathbf{m}_k) + \mathbf{J}_k(\mathbf{m}_{k+1} - \mathbf{m}_k) \quad (6.9)$$

$\mathbf{J}_k = (\partial \mathbf{F} / \partial \mathbf{m})|_{\mathbf{m}_k}$ is the *sensitivity matrix* or Jacobi-matrix calculated for model \mathbf{m}_k . Discarding the term χ_*^2 and fixing λ , with the above linearization, a stationary point of equation 6.8 can be calculated for each iteration k , yielding a model \mathbf{m}_{k+1} which is dependent on λ . Iterative repetition of these calculations will presumably converge to a ‘final’ model and a ‘final’ data misfit χ_d^2 , which strongly depends on the choice for λ and can be highly different from the desired misfit χ_*^2 .

Employing conventional inversion algorithms, the operator is constrained to run this procedure for various λ until a reasonable trade-off between model structure and data misfit is achieved, eventually reaching a misfit close to the desired χ_*^2 . Following the here adopted OCCAM¹ method, first introduced by *Constable et al. [1987]*, λ is varied *within each iteration*, and finally that value of λ is taken, which’s response $\mathbf{F}(\mathbf{m}_{k+1}(\lambda))$ minimizes the data misfit χ_d^2 for the actual iteration (in early iterations, the condition $\chi_d^2 \sim \chi_*^2$ will not be met). Once the desired misfit is reached, in a second phase a significantly narrower range of values is tested for λ in following iterations. This should keep the misfit down at the desired level, while minimizing the model norm.

¹named after William of Occam, respectively his well-known ‘razor’: “It is vain to do with more what can be done with fewer.” (e.g. *Russell [1959]*)

6.3 CALCULATION OF SENSITIVITIES

The DATA SPACE OCCAM method, which is implemented in REBOCC, takes advantage of the circumstance that stationary points \mathbf{m}_{k+1} of equation 6.8 (again discarding χ_*^2) can be expressed as

$$\mathbf{m}_{k+1} - \mathbf{m}_0 = \mathbf{C}_m \mathbf{J}_k^T \beta_{k+1} \quad (6.10)$$

(Parker [1994]), where the N elements of the coefficient vector β_{k+1} correspond to distinct data elements and have to be determined solving $\partial U(\mathbf{m}_{k+1})/\partial \mathbf{m}_{k+1} = 0$, with the above identity inserted. This formalism leads to the inversion of $(N \times N)$ matrices (\rightarrow *data space*) instead of the usually much larger $(M \times M)$ matrices, which saves significant computer resources with regard to storage and time.

As magnetotelluric and geomagnetic transfer functions vary rather slowly in space and frequency, their sensitivities with respect to changes in the model can also be supposed to vary slowly and thus bear significant redundances. Therefore, the above sketched data space approach suggests that a reduced set of data *representers* α_{k+1} , e.g. for data of every i -th period and/or j -th station, together with a subset sensitivity matrix \mathbf{G}_k should yield comparable results, if inserted in equation 6.10 instead of the term $\mathbf{J}_k^T \beta_{k+1}$. To solve the inverse problem ($\partial U(\mathbf{m}_{k+1})/\partial \mathbf{m}_{k+1} = 0$), the subset sensitivity matrix then has to be interpolated to the full sensitivity matrix by an interpolation scheme (which does not have to be very sophisticated), realized by a matrix \mathbf{B} :

$$\mathbf{J}_k = \mathbf{B} \mathbf{G}_k \quad (6.11)$$

From the implementation of this method, the name of the program is derived: REBOCC stands for REduced Basis OCCam inversion.

6.3 Calculation of sensitivities

The described inversion scheme is independent of the transfer functions that are to be inverted. The released version of REBOCC is capable to invert for apparent resistivities and phases of both, TE- and TM-mode, and for real and imaginary parts of local geomagnetic tipper functions ('TP', physically also TE-mode). Implicitly, the data type is reflected in the model response function \mathbf{F} , and as it is its basis, in the sensitivity matrix \mathbf{J} . To incorporate the inversion of inter-station transfer functions, the calculation of the model response function has to be modified just very little (see appendix A and below), but this has a major influence on the corresponding sensitivities and the calculation of these.

After linearization, the forward problem for one of the two modes reduces to the solution of an equation

$$\mathbf{K} \mathbf{v} = \mathbf{f} \quad (6.12)$$

where, for the TE-mode which will be considered here, \mathbf{v} is a vector consisting of the values for the electric field component in strike direction at *all* model nodes, and \mathbf{f} is a vector of the same length with the respective boundary conditions (the problem is formulated in a way that elements of \mathbf{f} referring to non-boundary nodes result to zero). \mathbf{K} is a multi-diagonal symmetric matrix which's elements bear most of the information on the model's dimensions

and resistivities. Linearization of the induction problem and thus construction of \mathbf{K} is performed as in *Apra et al.* [1997] and described in detail in appendix A.1. From the solution vector \mathbf{v} , the geomagnetic field at the earth's surface can be calculated, applying Maxwell's equation $\nabla \times \mathbf{E} = -i\omega\mathbf{B}$. This is explicitly shown in appendix A.2.

Sensitivities are the first derivatives of the data d obtained by forward calculation with respect to the variable model parameters m (here: conductivities). In MT, as the absolute values of the fields are a function of time, data are always ratios between two field components. Every field component Q can be regarded as a scalar product of a coefficient vector \mathbf{a}^T and the solution vector \mathbf{v} of the induction problem for the respective mode (cf. A.15): $Q = \mathbf{a}^T \mathbf{v}$. Thus for the sensitivities of an arbitrary field component, we have (chain rule):

$$\frac{\partial Q}{\partial m} = \left(\frac{\partial \mathbf{a}^T}{\partial m} \right) \mathbf{v} + \mathbf{a}^T \left(\frac{\partial \mathbf{v}}{\partial m} \right) \quad (6.13)$$

Differentiation of equation 6.12 with regard to the model parameter m

$$\frac{\partial \mathbf{K}}{\partial m} \mathbf{v} + \mathbf{K} \frac{\partial \mathbf{v}}{\partial m} = \frac{\partial \mathbf{f}}{\partial m} \quad (6.14)$$

inserted in equation 6.13 yields:

$$\frac{\partial Q}{\partial m} = \frac{\partial \mathbf{a}^T}{\partial m} \mathbf{v} + \mathbf{a}^T \mathbf{K}^{-1} \left(\frac{\partial \mathbf{f}}{\partial m} - \frac{\partial \mathbf{K}}{\partial m} \mathbf{v} \right) \quad (6.15)$$

Taking a closer look to this equation, it can be seen that for the calculation of the sensitivity, the forward problem, i.e. the equation $\mathbf{y} = \mathbf{K}^{-1} \mathbf{x}$, where \mathbf{x} is replaced by the expression in brackets, has to be solved at every model node m . Yet, taking advantage of the symmetry of the matrix \mathbf{K} , the equation can be reorganized, so that the forward problem just has to be solved for all data points, which are usually significantly fewer than the number of model parameters (i.e. the inversion problem is under-determined):

$$\frac{\partial Q}{\partial m} = \frac{\partial \mathbf{a}^T}{\partial m} \mathbf{v} + \mathbf{K}^{-1} \mathbf{a} \left(\frac{\partial \mathbf{f}}{\partial m} - \frac{\partial \mathbf{K}}{\partial m} \mathbf{v} \right) \quad (6.16)$$

(*Rodi* [1976]).

- Sensitivities of magnetic transfer functions d_D .

Here, the data are given by the transfer functions $d_D = B_y/B_{y0} - 1$. It thus has to be calculated:

$$\begin{aligned} \frac{\partial d_D}{\partial m} &= \frac{1}{B_{y0}} \frac{\partial B_y}{\partial m} - \frac{B_y}{B_{y0}^2} \frac{\partial B_{y0}}{\partial m} \\ &= \frac{1}{B_{y0}} \left[\frac{\partial \mathbf{a}_y^T}{\partial m} \mathbf{v} + \mathbf{K}^{-1} \mathbf{a}_y \left(\frac{\partial \mathbf{f}}{\partial m} - \frac{\partial \mathbf{K}}{\partial m} \mathbf{v} \right) \right] \\ &\quad - \frac{B_y}{B_{y0}^2} \left[\frac{\partial \mathbf{a}_{y0}^T}{\partial m} \mathbf{v} + \mathbf{K}^{-1} \mathbf{a}_{y0} \left(\frac{\partial \mathbf{f}}{\partial m} - \frac{\partial \mathbf{K}}{\partial m} \mathbf{v} \right) \right] \end{aligned} \quad (6.17)$$

6.4 SYNTHETIC EXAMPLES

or, numerically more efficient:

$$\frac{\partial d_D}{\partial m} = \left(\frac{1}{B_{y0}} \frac{\partial \mathbf{a}_y^T}{\partial m} - \frac{B_y}{B_{y0}^2} \frac{\partial \mathbf{a}_{y0}^T}{\partial m} \right) \mathbf{v} + \mathbf{K}^{-1} \left(\frac{1}{B_{y0}} \mathbf{a}_y - \frac{B_y}{B_{y0}^2} \mathbf{a}_{y0} \right) \left(\frac{\partial \mathbf{f}}{\partial m} - \frac{\partial \mathbf{K}}{\partial m} \mathbf{v} \right) \quad (6.18)$$

Note, that the first term in brackets of the second addend is independent of the model parameter m , and the second term in brackets is independent of the specific data type of the TE-mode. The coefficient vectors \mathbf{a}_y and \mathbf{a}_{y0} are mostly zero (cf. equation A.15), and for model parameters where $\partial \mathbf{a}_y^T / \partial m$ is unequal zero, the term $\partial \mathbf{a}_{y0}^T / \partial m$ will be zero and vice versa, since site and reference site (or: node) are in general not side by side.

- Sensitivities of magnetic transfer functions z_D .

Here, the data are given by $z_D = B_z / B_{y0}$. Completely analogous, we obtain:

$$\frac{\partial z_D}{\partial m} = \left(-\frac{B_z}{B_{y0}^2} \frac{\partial \mathbf{a}_{y0}^T}{\partial m} \right) \mathbf{v} + \mathbf{K}^{-1} \left(\frac{1}{B_{y0}} \mathbf{a}_z - \frac{B_z}{B_{y0}^2} \mathbf{a}_{y0} \right) \left(\frac{\partial \mathbf{f}}{\partial m} - \frac{\partial \mathbf{K}}{\partial m} \mathbf{v} \right) \quad (6.19)$$

with $(\partial \mathbf{a}_z / \partial m = 0)$, compare equation A.17 in appendix A.2).

Having implemented these sensitivities, with some slight additional changes as calculation of the new forward responses and in- and output, the program can now invert up to five data types (nomenclature as used in the program): TE & TM (ρ_a & ϕ of the two modes), TP (real and imaginary parts of the local magnetic transfer function T_y), and d_D & z_D (both also real and imaginary parts).

6.4 Synthetic examples

Geomagnetic perturbations \mathbf{W} , as introduced by *Schmucker* [1970], have been thought as a means to quantitatively describe *anomalous* geomagnetic variations with respect to a defined, not necessarily purely horizontal *normal* variation, which is either observed at a chosen reference or deduced synthetically as the average magnetic field of a certain number of sites.

Schmucker [1993] inverted for an with respect to a normal 1-D background resistivity $\sigma_N(z)$ anomalous two-dimensional conductivity distribution $\sigma_a(y, z)$, employing a finite element algorithm. His input data were anomalous *fields*, calculated from local TE-mode impedances and tipper data of a subset of the COPROD2 (see *Jones* [1993]) data set and responses from the estimated 1-D background conductivity distribution:

$$E_{xa} = Z_{xy} / Z_N \cdot (1 + B_{ya}) \quad (6.20)$$

$$B_{za} = T_y (1 + B_{ya}), \quad B_{ya} = B_y - B_{y0} \quad (6.21)$$

Leibecker [2000] made the suggestion to develop a local, two- or three-dimensional model which sufficiently well explains the *local* data at the reference station, to which the geomagnetic field of all other stations is related. Calculating a synthetic perturbation of the field from the reference with regard to a synthetic normal site far away from any anomalies of the model, final perturbations can be calculated between all field sites and the synthetic, true

one-dimensional normal field. Though the model does not have to be very sophisticated and though it only has to explain the data of one site, it has to be constructed before the full modelling and it should not be too far from the true conditions.

The wish to relate all fields to a true normal reference corresponds to the request, that all perturbation data shall be related to an *anomalous* conductivity distribution σ_a , and this only via the local fields (e.g., for a 2-D conductivity distribution: $B_y(\sigma_a) - B_{y0} = d_D(\sigma_a) * B_{y0}$). For data where this condition cannot be met, forward modelling might be very difficult. As an inversion scheme is presented here, considerations on uniqueness instead of instructiveness get more important, and, as could have been seen above, the responses are sensitive to fields of both, local site and reference. At this point, an additional deliberation arises: Especially for d_D , one could request that the data should *equally* depend on changes of the fields at the local site and at the reference, respectively of the conductivities below them. This would easily be achieved by inverting $\ln(B_y/B_{y0}) = \ln(B_y) - \ln(B_{y0})$ instead of d_D . If this suggestive but completely unusual change of the data type would further improve the inversion results shown below has still to be tested.

For the following two synthetic examples, joint inversion results of combinations of modes, as presented in *Siripunvaraporn and Egbert* [2000] will not be shown here, as only the physics of the single data types for the respective models shall be studied. For all inversion calculations presented below, the data subset of every second period at all stations was chosen for the calculation of the subset sensitivity matrix, which is interpolated to the full sensitivity matrix (see section 6.2).

6.4.1 Model from Siripunvaraporn & Egbert

The first model that the code is tested with for the new features, is taken from *Siripunvaraporn and Egbert* [2000], who in turn derived it from inversion results of the COPROD2 data set (cf. *Jones* [1993]) from *Wu et al.* [1993]. It is a four layered model (100 Ω m: 0–10 km, 1000 Ω m: 10–40 km, 100 Ω m: 40–100 km, 10 Ω m: 100– ∞ km), with three quadratic highly conductive (1 Ω m) anomalies (A, B & C) in the resistive second layer. The side-lengths of the anomalies are (from left to right) 15 km, 20 km and 10 km, and they are buried at 15 km, 20 km and 25 km depth, separated by 20 km and 10 km, respectively (see figure 6.1). On top of the model are 36 stations with a spacing of 3 km, plus – in contrast to *Siripunvaraporn and Egbert* [2000] – an additional station, which serves as a reference for transfer functions d_D and z_D , situated 40 km left of the second station and 55 km left of anomaly A. The synthetic input data for the inversion calculations have been generated with the finite element code from *Wannamaker et al.* [1987], using a discretization of 374 rows and 86 columns, with 10 additional air layers for the TE-mode. Periods range logarithmically equidistant from 1 s to 1000 s, with 10 periods per decade. Two percent Gaussian noise was added to the synthetic data, which shall mean that the errors of the data are set to

$$\Delta\rho^{\text{TM,TE}} = 0.02 \cdot \rho_a^{\text{TM,TE}}, \quad \Delta\phi^{\text{TM,TE}} = 0.02 \cdot 90/\pi \quad (6.22)$$

$$\Delta\Re(T_y, d_D, z_D) = 0.01, \quad \Delta\Im(T_y, d_D, z_D) = 0.01 \quad (6.23)$$

6.4 SYNTHETIC EXAMPLES

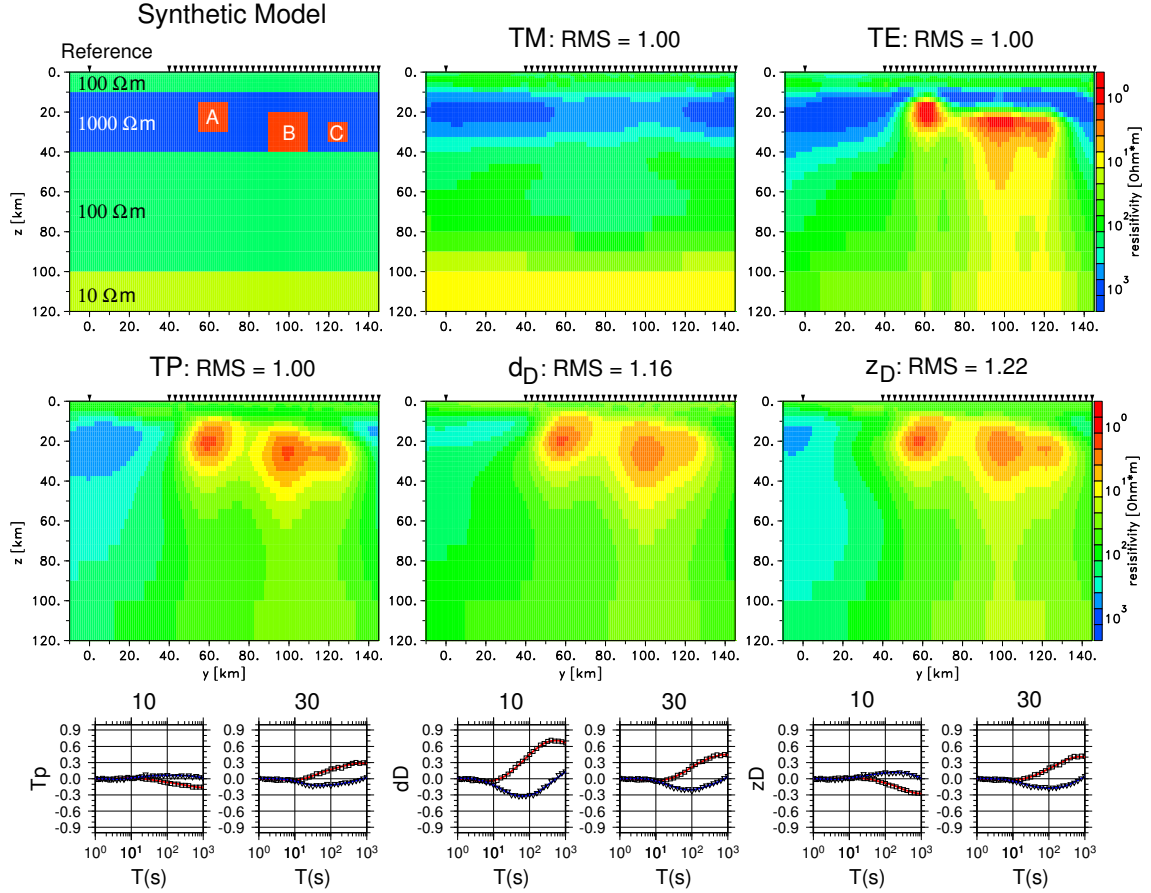


Figure 6.1: Synthetic model as in Siripunvaraporn and Egbert [2000] with three conductivity anomalies A, B & C of $1\Omega\text{m}$ in the resistive second layer and five models, resulting from inversions of apparent resistivities and phases of the two modes (TM, TE), real and imaginary parts of local tipper functions $T_y = B_z/B_y$ (TP) and the in this version additionally invertible transfer functions $d_D = B_y/B_{y0} - 1$ and $z_D = B_z/B_{y0}$. Reference is the leftmost station. For the latter three data types, also data (black) and responses (colored; red: real parts, blue: imaginary parts) of stations 10 and 30 (numbered from left upwards) are shown.

and the data itself were modified, subtracting a value according to the above error, whereat the number 0.02 (0.01) was replaced by a normal distributed random number of standard deviation 0.02 (0.01).

For the inversion, a homogeneous start and prior model of $100\Omega\text{m}$ resistivity was chosen, with a discretization of 187×43 elements, i.e. two times coarser than in the forward modelling. Figure 6.1 shows inversion results of apparent resistivities of the two modes (TM, TE), real and imaginary parts of local magnetic transfer functions (TP) and the newly invertible transfer functions d_D (anomalous horizontal magnetic field) and z_D (local vertical magnetic field related to the horizontal magnetic field of the reference). Inversions of local transfer functions converged completely (i.e. $\text{RMS} = 1.00$), whereas for transfer functions d_D and z_D the achieved minimum RMS was 1.16 and 1.22, respectively. Obviously, currents within the model plane are very little deflected by the three anomalies A, B & C, and the TM-

mode inversion basically reflects the one-dimensional background resistivities. In contrast, inversion of apparent resistivities and phases of the TE-mode (TE) best recover the overall conductivity distribution. Inversions of T_y (TP), d_D and z_D yield comparable models, with a slightly diminishing quality from TP via z_D — both these inversions reconstruct the three anomalies — to d_D , where the vertical and lateral boundaries are poorly resolved.

Looking at the sample transfer functions of stations 10 and 30 (numbering from left upwards) for the three data types, we see that above the leftmost anomaly A the horizontal magnetic field increases by a factor > 1.6 (i.e. $d_D > 0.6$), and as a consequence, the transfer function T_y (TP) is diminished with respect to z_D , as the local horizontal magnetic field is in its denominator. It can be argued that extending the period range towards longer periods, inversions of data that physically belong to the TE-mode (TE, TP, d_D , z_D) would better resolve deeper conductivities and lower boundaries of the anomalies, since the real parts of the shown magnetic data are still close to their extremal values at 1000 s.

6.4.2 A very crude ANCORP resistivity model

From the results of *Schwalenberg* [2000] (see also: *Brasse et al.* [2002]), which were obtained by 2-D inversion of apparent resistivity and phase data of 30 stations from the ANCORP-profile, and from the forward modelling studies presented in *Soyer and Brasse* [2001], fitting the transfer functions d_D and z_D , a very crude, schematic conductivity distribution for the ANCORP-profile was derived, which's features are not subject to discussion here.

The model is divided into two ‘quarter-spaces’ of 300 Ωm (left) and 100 Ωm (right), with the following conductivity anomalies inserted (see figure 6.2): The Pacific ocean is simulated by a highly conductive 4 km deep block of 0.27 Ωm , extending to $-\infty$ towards west. The Pre-cordillera anomaly is represented by a nearly quadratic structure of ~ 9 km side-length and 1 Ωm conductivity, buried at only 4 km depth. On the eastern side, a 2,5 km thick sheet of superficial high conductivities (1 Ωm), which extends approximately 140 km in E-W direction, is placed at a depth of 500 m, representing sediments on the Altiplano. At 15 km depth, a 1 Ωm sheet of 8 km thickness and ~ 170 km lateral extension, together with a domain of 3 Ωm below, which reaches down to 65 km depth, characterizes the Altiplano high conductivity anomaly. To numerically stabilize the forward responses, the top layers comprising the upper 100 m were set to a conductivity of 1 Ωm .

The locations of the 35 stations are the same as for the field sites, with a spacing of approximately 10 km. Also, the periods are identical with the target frequencies of the processing of real data, ranging from ~ 10 s to $\sim 23,000$ s with 8 periods per decade.

Forward modelling was again performed with the code from *Wannamaker et al.* [1987], here with a discretization of 392 columns and 100 rows. For the calculation of the transfer functions d_D and z_D , the horizontal magnetic field of the sixth station, which represents CTE, was defined as ‘normal’ and served as reference. As in the previous section, data of the single types were inverted independently: ρ_a & ϕ of the two modes (TM, TE), real and imaginary parts of local geomagnetic transfer functions (TP), and the inter-station transfer functions d_D and z_D . As above, two percent noise was added to the data.

6.4 SYNTHETIC EXAMPLES

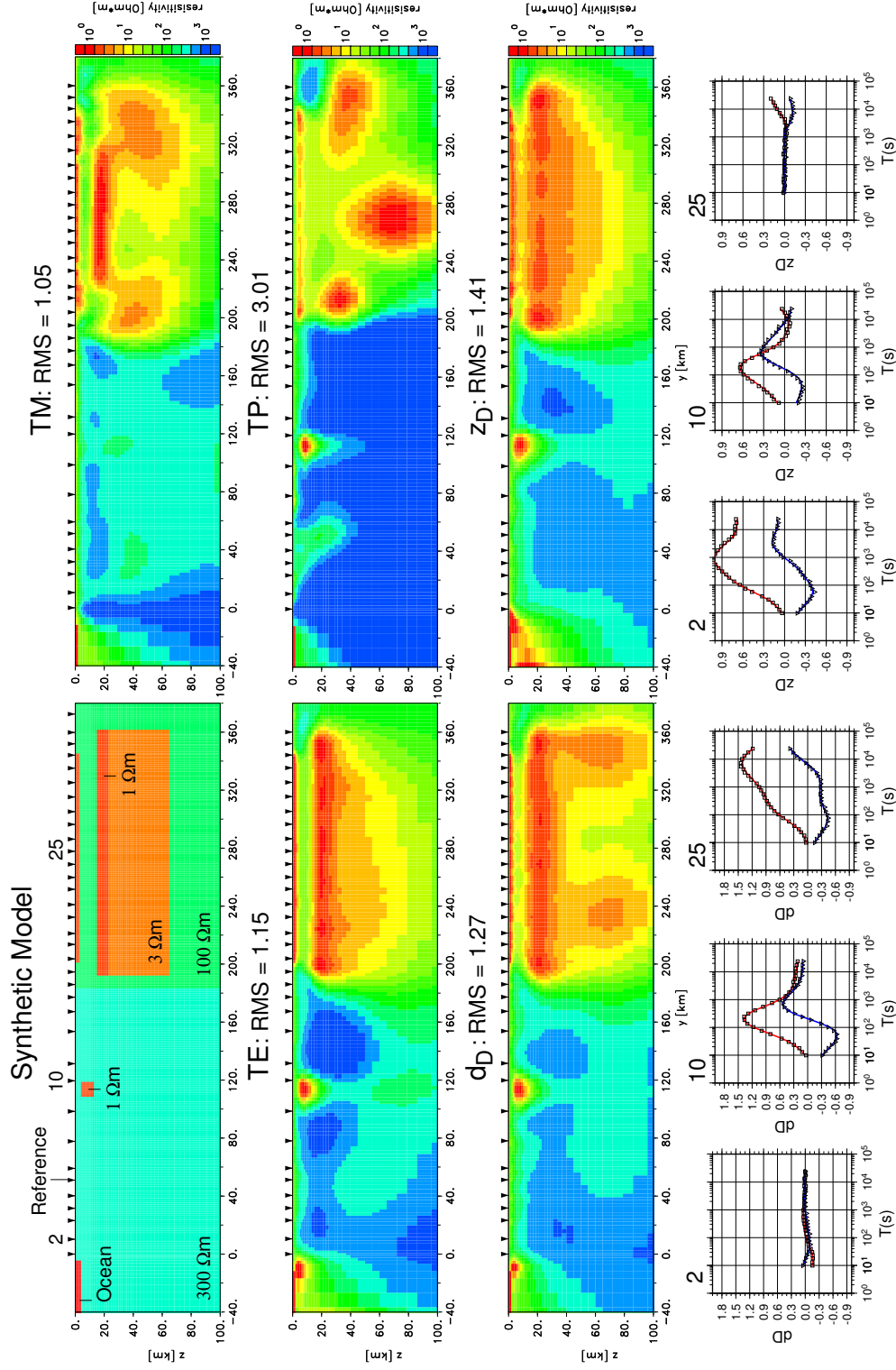


Figure 6.2: A very crude ANCORP resistivity model, derived from the $(\rho_u$ & ϕ) 2-D inversion results of Schwaberg [2000] and forward modelling studies, fitting the inter-station transfer functions d_D & z_D (Soyer and Brasse [2001]), and inversion results for the five possible data types (for explanation see caption of figure 6.1 and text). For d_D and z_D , synthetic data and responses at three characteristic stations (close to the ocean, above the Precordillera anomaly and on the Altiplano) are shown.

In the inversion, discretization was twice as coarse as that for the generation of the synthetic data, using 196×50 elements. Start and prior models were $100 \Omega\text{m}$ half-spaces with the ocean included, which was fixed during inversion. Inversions of apparent resistivities and phases of TM and TE-mode converged best (RMS = 1.05 & 1.15), followed by the inversions of inter-station magnetic transfer functions d_D and z_D (RMS = 1.27 & 1.41). Surprisingly, inversion of local magnetic transfer functions T_y (TP) did not converge (RMS = 3.01). The high conductive uppermost 100 meters (see above) are obviously reflected in all inversion results by downward increasing resistivities within the upper ~ 10 km on the western part of the models (see figure 6.2). Comparable to the previous section, the Precordillera anomaly, being a high conductivity anomaly of small extension within a resistive host which does not reach to the surface, has minor influence on superficial apparent resistivities of the TM-mode and is thus not found in the inversion results. In contrast, all models from inversions of transfer function that physically belong to the TE-mode (i.e. the other four) show this anomaly very well. The overall conductivity distribution is again best recovered by inversion of apparent resistivities and phases of the TE-mode.

Conductivity distribution in the eastern part of the model is locally approximately one-dimensional, and rather than to resolve the lateral structure of the anomalies as in the previous section, the task of any inversion here is to reconstruct the vertical structure. As the vertical magnetic field is about zero above the center of the anomaly for a wide period range, transfer functions with B_z in their nominator have no information on any vertical conductivity distribution, resp. they only do contain the information that *locally* no lateral variation of conductivity is observed (see z_D of site 25, figure 6.2). In contrast, the local anomalous horizontal magnetic field has ‘full’ signature of the 1-D conductivity distribution below (see d_D of site 25, with values > 1.2 , i.e. $B_y > 2.2 \cdot B_{y0}$). As a consequence, the resistivity distribution below the ‘Altiplano’ is much better recovered by inversion of d_D than by inversion of local geomagnetic transfer functions T_y (TP) or z_D , inversion of the former even failed to converge. Close to the ocean, the opposite effect is observed: The horizontal magnetic field is just slightly decreased onshore, whereas the vertical magnetic field partly even equals the horizontal field (i.e. $T_y = 1$, cf. transfer functions d_D and z_D of site 2). This will be discussed in more detail in section 7.1.

6.4.3 Inversion of data with various references

In practice, it can be difficult to relate the measured field of all stations to that of one chosen reference, or eventual calculations to successively combine sub-arrays may lead to contamination of good data due to bad local data of the important overlapping station(s). For such cases, one might want to have the possibility to invert inter-station data where the field of each station is related to that of an individual reference, i.e. at station i :

$$d_D^i = \frac{B_{yi}}{B_{y0}} - 1 \quad \Rightarrow \quad d_{Dj(i)}^i = \frac{B_{yi}}{B_{yj(i)}} - 1 \quad (6.24)$$

(z_D analogous). The necessary extension of the code to invert such data is trivial and at most a task in terms of data organization: besides the calculation of these transfer functions from the fields of the forward modelling, B_{y0} in equations 6.18 and 6.19 has to be replaced by $B_{yj(i)}$ in the calculation of the sensitivities. As shown above, the speciality of the *reduced*

6.4 SYNTHETIC EXAMPLES

basis data space OCCAM approach is that the full sensitivity matrix is calculated via interpolation from a smaller matrix containing sensitivities at a chosen subset of data. This interpolation is normally done between values from adjacent periods and stations. Using various references, the interpolation between stations has to be omitted, since now sensitivities cannot be supposed to vary smoothly in space.

Yet, the question on the uniqueness of inversion solutions is of different quality here: Imagine a two-dimensional model which's conductivity distribution is symmetric with regard to the axis $y = 0$ (cf. figure 6.3 for illustration). Then, a transfer function $d_D(y) = B_y(y)/B_y(-y) - 1$ will be identically zero for any y and the only information on the subsurface conductivity is that it must be symmetric with respect to $y = 0$. It might however be that for ideal, continuous data as in section 6.1.2 without symmetric organization, a theorem on uniqueness resp. invertability can be deduced as well.

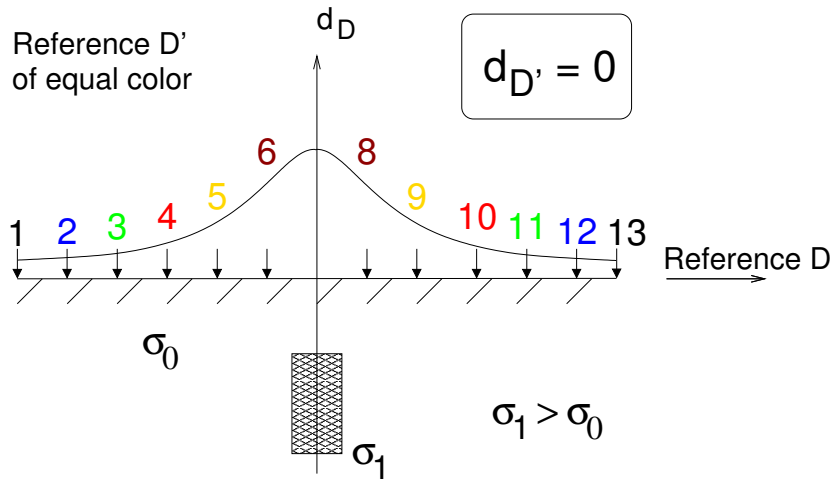


Figure 6.3: Over a symmetric model, the transfer function d_D with a reference far away from conductors is also symmetric. Thus, a transfer function $d_{D'}$ which relates the horizontal field to that of the ‘mirror’ site (in this example by grouping equal colors, so that the sum of station numbers results to 14) wipes out any information on the anomalous conductivity.

The inversion with various references has also been tested with synthetic data, which were generated from the two models of the previous section in the same manner as above. To check if such an inversion does work at all, a quite complex, random resp. associative site – reference site combination schema was chosen (table 6.1).

Figure 6.4 shows inversion results for transfer functions d_D of the model from *Siripunvaraporn and Egbert* [2000]. Though the convergence is very good, the inversion badly reconstructs the original conductivity distribution. As is clear and has been verified in the previous section, transfer functions d_D between stations above and far away from conductors have generally the highest absolute values. The site – reference site combinations from table 6.1 for this model, however, lead to a set of data, where this is only realized for data from two stations (1 & 17), and data from all other stations are of small value. This is also reflected in a much smaller starting RMS at the beginning of the inversion.

Site	1	2	3	4	5	6	7	8	9	10	11	12	13
Ref.	18	5	33	7	21	11	25	36	34	15	2	28	31
Site	14	15	16	17	18	19	20	21	22	23	24	25	26
Ref.	3	22	6	1	27	17	8	32	26	12	14	4	37
Site	27	28	29	30	31	32	33	34	35	36	37		
Ref.	20	29	16	35	24	13	30	19	9	23	10		

Table 6.1: Site – reference site organization for data d_D , as they were calculated from the model of Siripunvaraporn and Egbert [2000]. Each station is only used once as reference.

For the inversion of data from the synthetic ANCORP model, the site and reference grouping was basically as in table 6.1 (changes only due to the smaller number of stations). Here the model is recovered very well, which is surely due to the circumstance that for a sufficient number of sites on the ‘Altiplano’, the respective references lie westward of the major anomalies, where only the – also well recovered – ‘Precordillera’ anomaly is situated (see figure 6.5).

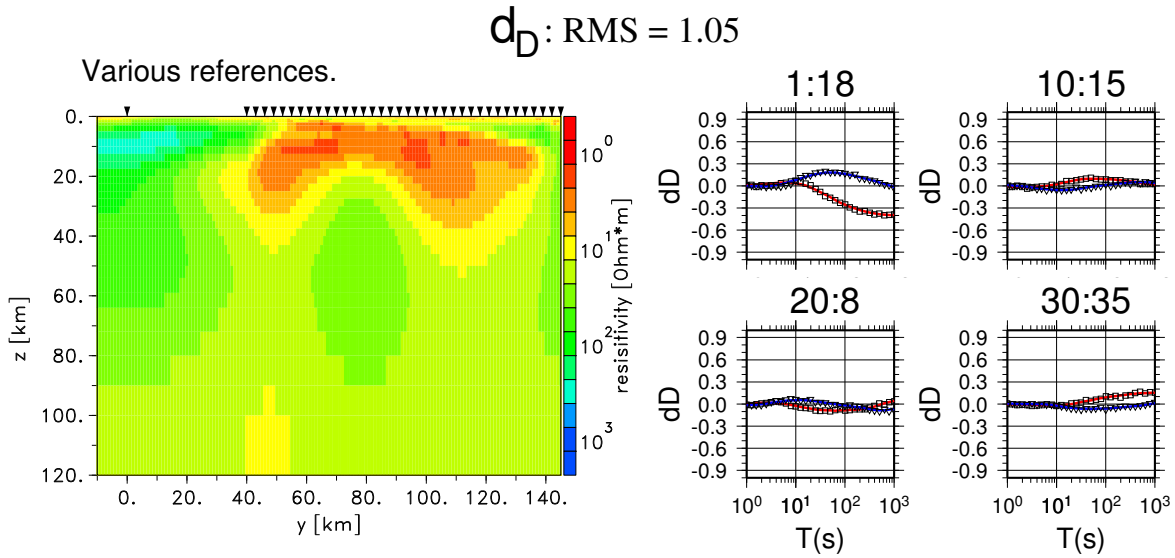


Figure 6.4: Results from the inversion of data d_D from the synthetic model shown in figure 6.1, with the ‘random’ site – reference site relations from table 6.1.

6.4 SYNTHETIC EXAMPLES

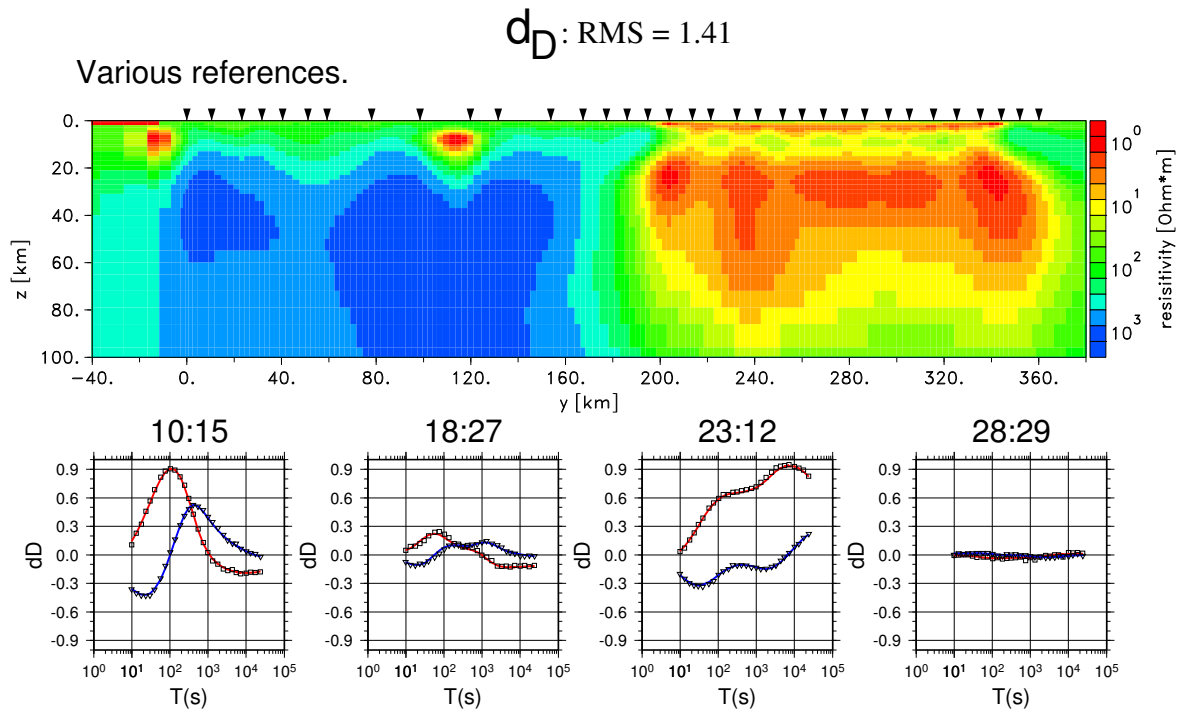


Figure 6.5: Inversion results from transfer functions d_D of the synthetic, schematic ANCORP model (figure 6.2), with a site and corresponding reference grouping almost identical with that of table 6.1.

